Discovery of diminazene as a dual inhibitor of SARS-CoV-2 host target proteases TMPRSS2 and furin using cell-based assays

Ya-Ming Xu, Marielle Cascaes Inacio, Manping X. Liu, and A. A. Leslie Gunatilaka*

Southwest Center for Natural Products Research, School of Natural Resources and the Environment, College of Agriculture and Life Sciences, University of Arizona, Tucson, Arizona 85706, United States

Supplementary Material

Table of Contents

Figure S1. The effect of cell density (cells/well) of VeroE6/TMPRSS2 overexpressing cells on fluorescence intensity

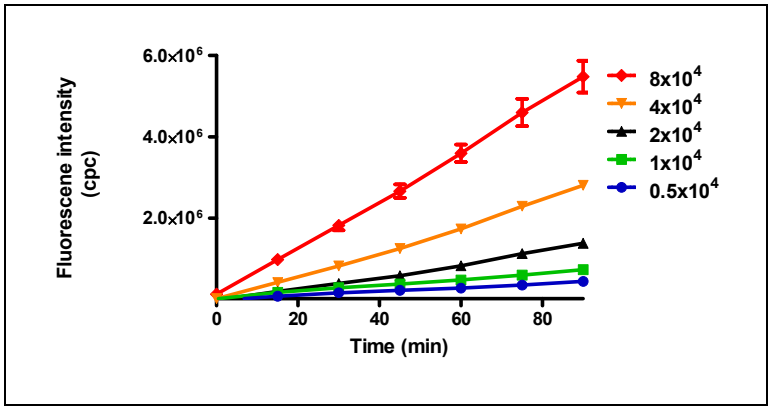

Figure S2. TMPRSS2 enzyme activity comparison of VeroE6/TMPRSS2 overexpressing cells and LNCaP cells (substrate concentration = 50 μM)

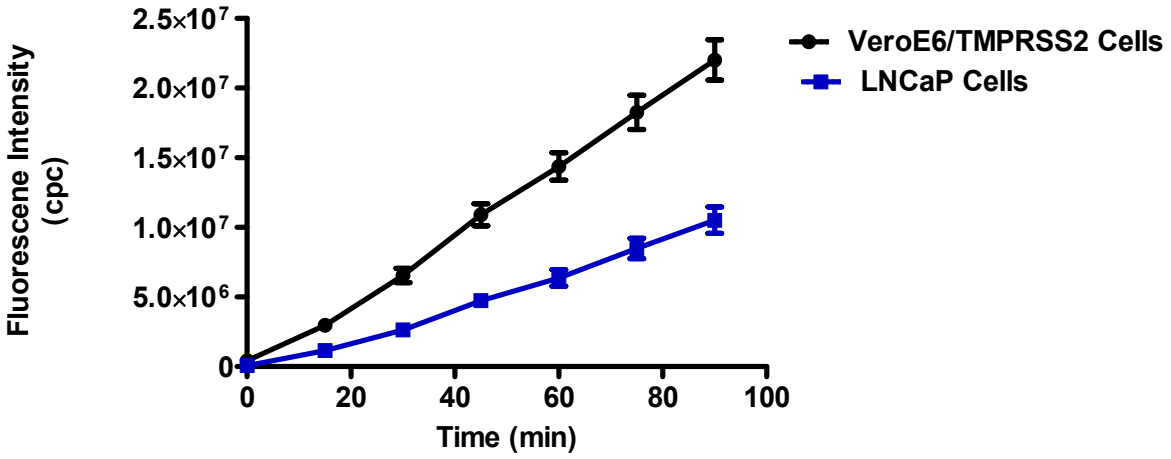

Figure S3. TMPRSS2 enzyme activity comparison of VeroE6/TMPRSS2 overexpressing cells and VeroE6 cells (substrate concentration = 100 μM)

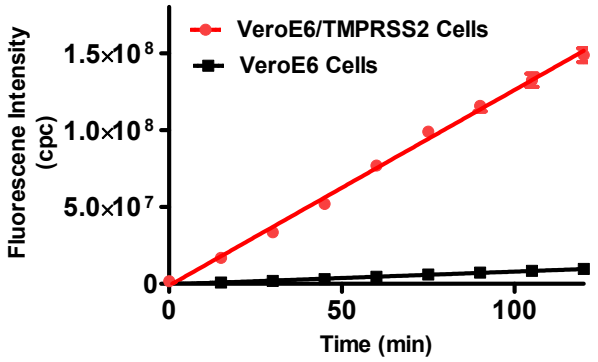

Figure S4. Comparison of furin enzyme activity of Vero cells overexpressing furin in cells (with detergent, Tween 20, and without detergent, Tween 20) and the medium (substrate concentration = 100 μM)

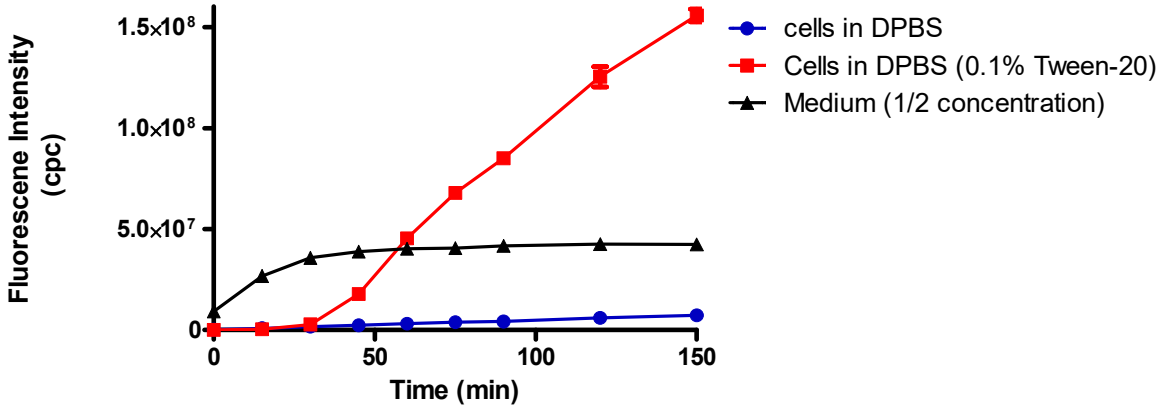

Figure S5. Furin enzyme activity comparison of Vero/furin overexpressing cells and VeroE6 cells

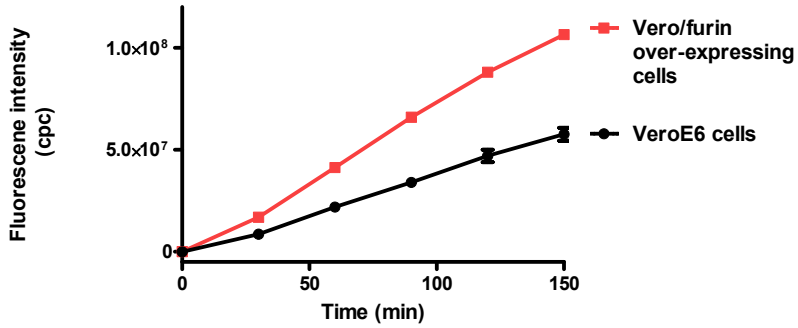

Figure S6. Furin substrate titration and kinetic data. (**A**) Furin substrate titration curves. (**B**) Kinetic data from Figure A were plotted to estimate the *K*m by curve fitting of the Michaelis–Menten equation (K_m=44.6 μM). The initial rate were calculated based on the data of 30-60 min time period. Curve fitting was carried out using GraphPad Prism. Error bars indicate the standard error of the mean.

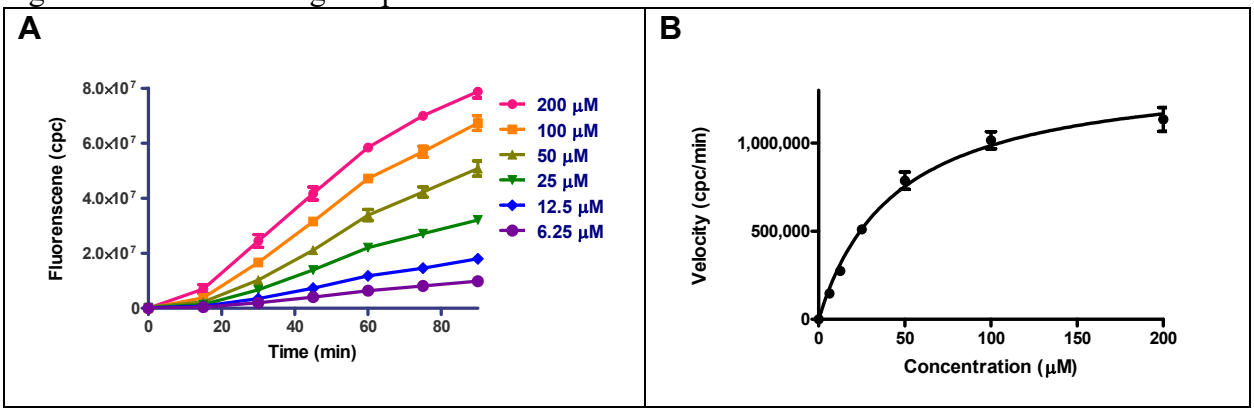

Figure S7. The effect of cell density of Vero/furin overexpressing cells on fluorescence intensity

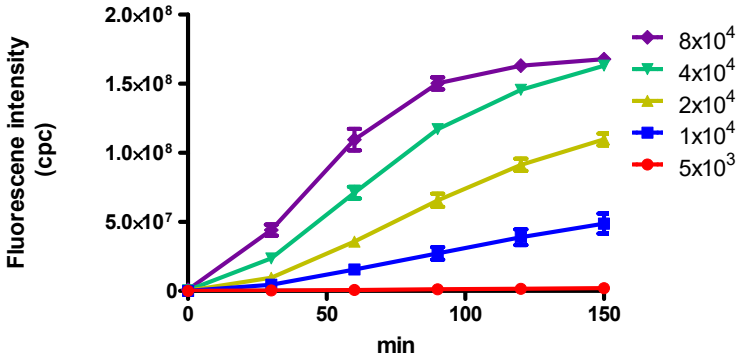

8. Molecular Docking Studies

TMPRSS2

TMPRSS2 protein model

Due to the unavailability of TMPRSS2 crystal structure, we used its homology model obtained from the Universal Protein Resource, UniProtKB, database (UniProt id = O15393) and homology modelling performed by template-based method on the Swiss-Model (https://swissmodel.expasy.org/). The protein used as template is the transmembrane serine protease hepsin [PDB code 1z8g, chain A, X-ray diffraction with 1.55 Å resolution, sequence identity = 33.62% to target sequence; sequence similarity = 38%, sequence coverage = 71%, amino acids range = 144-191 (extracellular region residues), QMEAN score = -1.82, model-template alignment RMSD = 0.4 Å]. The quality of the model was also analyzed using ERRAT[1] (83.83%) and by generating Ramachandran plots on PROCHECK[2] (84.7% of the residues in most favored regions and 14.9% in allowed regions), both calculated through the online server Saves v6.0 (https://saves.mbi.ucla.edu/).

Preparation of receptor, ligands and molecular docking

The protein file was opened in the Swiss-pdbViewer[3] to check and correct the possible errors found in the amino acids chain and remove water. The quality of the protein was again analyzed using the same procedure cited above. The catalytic site of the enzyme was checked for the presence of the triad residues HIS296, ASP235 and SER441.[4–6] AutoDock tools 1.5.6 was used to add polar hydrogens and the protein was saved in *.pdbqt format.

Camostat, a known TMPRSS2 inhibitor[7,8] was used to compare the results with diminazene. For the preparation of ligand structures, 2D structures was sketched with the MarvinSketch where the pKa was calculated in the physiological pH (7.4) (the molecules were protonated in the guanidinium groups) and converted to 3D models. Molecular geometry optimization was made using MOPAC2016 and the structures were saved in *.mol2. Charges were added to the structures by loading them in the UCSF Chimera 1.15[9] and saved as *.pdb format. Structures were then checked for the addition of Gasteiger charges and torsions with AutoDock tools and saved in *.pdbqt format.

Molecular docking was carried out using AutoDock Vina 1.1.2 at an exhaustiveness of 8. Grid box parameters were set to cover the catalytic site of TMPRSS2, covering the triad HIS296, ASP345 and SER441 residues and its adjacent residues. The box was centered at $X = 31.5774$, Y

= -1.31236, *Z* = 30.0788, with a grid box dimension of 24.2486 Å x 19.696 Å x 21.2 Å. Re-docking into the same dimensions were made to validate the results. The protein-ligand interaction results were analyzed using Protein-Ligand Interaction Profiler (https://projects.biotec.tu-dresden.de/plip-web/plip) and visualization of binding pose was done using Pymol 2.3.4. The graphical depictions of ligand-protein complexes were also plotted by UCSF Chimera.

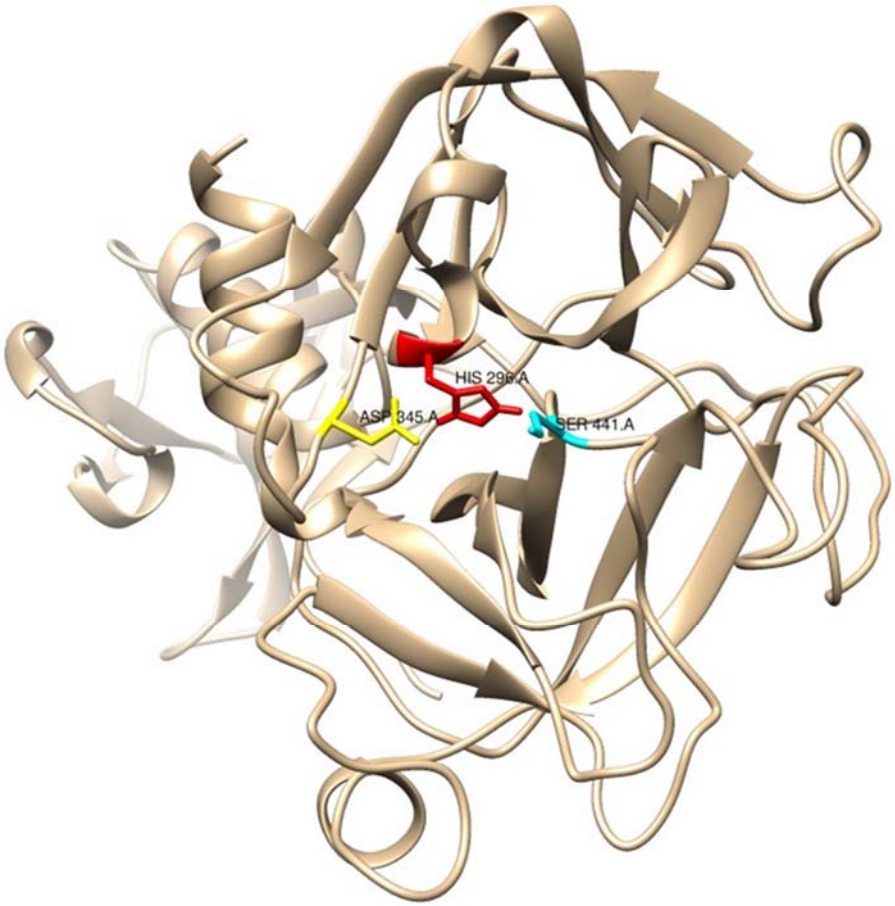

Figure S8-1. TMPRSS2 structure containing the triad residues HIS296 (red), ASP345 (yellow) and SER441 (cyan) forming TMPRSS2 active site.

Table S8-1. Protein-ligand binding energy and interactions generated from molecular docking using AutoDock Vina.

	Diminazene	**Camostat**
Binding energy (kcal/mol)	-6.7	-6.7
Hydrophobic interactions – residue (distance Å)	VAL280 (4.00), THR (3.57)	VAL280 (3.90), GLN438 (3.68)
Hydrogen bond – residue (distance Å)	HIS296 (2.63 and 2.81), SER436 (3.43 and 1.88), GLN438 (2.48), GLY439 (2.99), SER441 (2.82), SER460 (2.38), GLY464 (1.94)	HIS279 (2.34), VAL280 (2.86), SER436 (2.85), GLN438 (3.26), SER441 (2.16), SER460 (3.61)
π-Stacking	HIS296 (4.45)	-
Salt bridges	-	HIS296 (4.74)

FURIN

Furin protein model and docking softwares

The crystal structure of furin (PDB code 5JXH) was used for docking experiments. Three software using different algorithms were used: Autodock Vina[10] (rigid docking), SwissDock[11] (blind docking) and DockThor[12] (flexible-ligand and rigid-receptor). More information about the details of each one can be found in the references. For the experiments done using AutoDock Vina, protein and ligands were prepared as described above for TMPRSS2. For the free web-based docking software SwissDock and DockThor, protein and ligands were prepared according to their instructions. Grid box size around active site were kept similar as much as possible. Blind docking uses the whole protein.

Comparison of software and ligands

The binding energy value obtained for each compound was different depending on the software/algorithm used (Table S8-2) and in some cases does not represent experimental results.

That discrepancy between computational studies and experimental data are frequently found in literature, especially for virtual screening, in which hundreds of compounds were found as having good binding energy through molecular docking, but only a few of them were really active in *in vitro* experiments.[13–15] Based on the scores, DockThor with soft docking activated seems to be the best option, from which the lowest binding energy was obtained for diminazene although binding energy does not necessarily represents biological activity.[13]

Table S8-2. Estimated binding energy (kcal/mol) of the compounds diminazene, camostat and nafamostat in interaction to furin (PDB code 5JXH) using different software.

Software	Diminazene	Camostat	Nafamostat
Autodock Vina	-7.8	-7.8	-9.2
SwissDock	-13.24	-11.10	-13.84
DockThor soft*	-18.23	-12.76	-7.31
DockThor non-soft*	-9.36	-1.60	-10.88
DockThor blind soft*	-13.30	-3.70	-15.18

* Soft Docking implicitly considers the protein flexibility; non-soft docking uses an empirically determined softening constant.

The figure S8-2 shows that diminazene specifically binds at the same site independently of the software used and in very similar binding poses (in the catalytic/binding site according to literature[16–18] containing the key residues ASP153, HIS194, SER368, LEU227 and TRP254). Camostat and nafamostat can also bind in different sites and/or poses. These results show that diminazene has more affinity for the active site than the other compounds. The bindings in different places/or non-active pockets mean the reduced opportunity to bind to active site, which may also explain the less active or not active against furin for camostat and nafamostat.

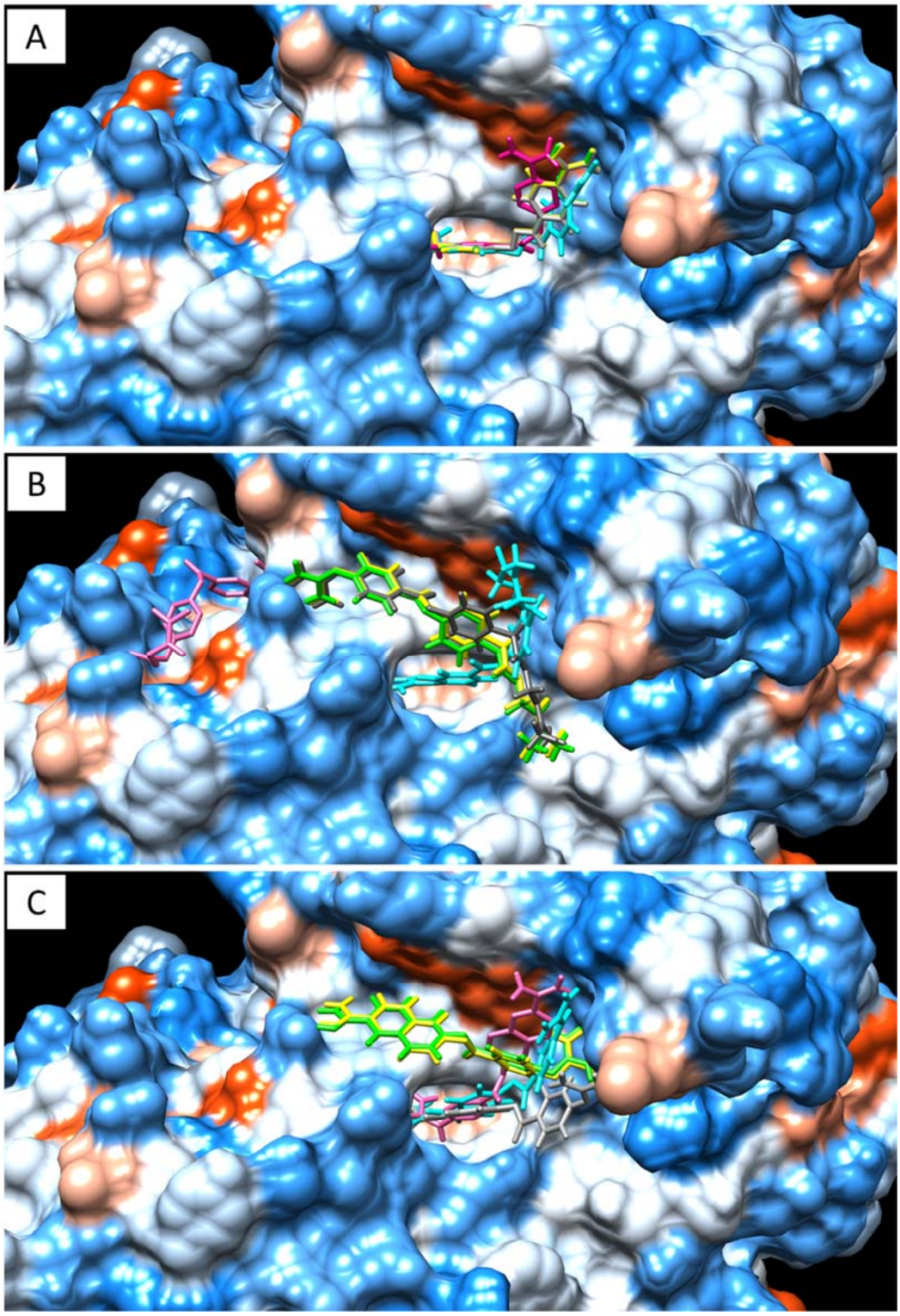

Figure S8-2. Poses of the compounds in the lowest-energy binding using different software. (**A**) diminazene. (**B**) camostat. (**C**) nafamostat. Autodock Vina results is showed in pink; SwissDock in cyan; DockThor soft* in yellow; DockThor non-soft* in green; DockThor blind soft* in dark grey. *Soft Docking implicitly considers the protein flexibility; non-soft docking uses an empirically determined softening constant. Protein is in the same orientation.

To evaluate the interactions, the results obtained from AutoDock Vina and DockThor soft were selected. AutoDock Vina showed the lowest energy binding for nafamostat while DockThor soft showed the best score for diminazene (Table S8-2). The number of favorable interactions (H-bonds and hydrophobic interactions) is higher for diminazene than for the other compounds when DockThor soft was used. The favorable interactions occur with residues from the catalytic triad and binding site (Table S8-3). Interactions of diminazene with the residues LEU227, ASP258, ASP306 were previously related.[16] When AutoDock Vina was used, nafamostat showed more favorable interactions than diminazene (11 and 10, respectively). However, diminazene interacts with a higher number of residues from the catalytic/binding site (Table S8-3).

Table S8-3. Protein-ligand interactions generated from molecular docking using DockThor and AutoDock Vina (Distance in Å is showed between parentheses).

	Hydrogen bonds				**Hydrogen bonds**		
DockThor soft	Diminazene (6)	Camostat (3)	Nafamostat (5)	AutoDock Vina	Diminazene (7)	Camostat (3)	Nafamostat (7)
	ASN192 (3.08)	-	-		-	-	-
	LEU227* (3.22)	-	-		LEU227* (2.41, 2.72)	-	LEU227 (2.94)
	SER253 (2.55)	-	-		-	-	-
	ASP258* (1.72)	-	-		-	-	-
	ASP306* (1.71)	-	ASP306 (3.06, 1.83)		ASP306* (2.30)	-	-
	SER368 (3.46)	SER368 (1.83)	-		SER368 (2.33, 3.32, 3.01)	-	-
	-	GLY255 (3.06)	-		-	-	-
	-	HIS194 (2.21)	-		-	-	-
	-	-	ASP191 (1.85, 2.23)		-	-	-
	-	-	ASN295 (2.81)		-	-	ASN295 (3.35)
	-	-	-		SER293 (2.81)	-	-
	-	-	-		-	GLY307 (3.48)	-
	-	-	-		-	ARG498 (3.09)	-
	-	-	-		-	ASN529 (2.66)	-
	-	-	-		-	-	ASP228 (2.35, 3.18)
	-	-	-		-	-	PRO256 (2.39)
	-	-	-		-	-	TRP291 (3.15)
	-	-	-		-	-	ALA292 (2.59)
	Hydrophobic interactions				**Hydrophobic interactions**		
DockThor soft*	Diminazene (2)	Camostat (4)	Nafamostat (2)	AutoDock Vina	Diminazene (3)	Camostat (5)	Nafamostat (4)
	LEU227* (3.46)	LEU227 (3.51, 3.83)	-		LEU227* (3.46)	-	LEU227 (3.66, 3.82)
	THR367 (3.77)	-	THR367 (3.48)		THR367 (3.36)	-	THR367 (3.49)
	-	VAL231 (3.71, 3.92)	-		-	-	-
	-	TRP254 (3.87)	-		TRP254* (3.90)	-	-
	-	-	HIS194 (3.94)		-	VAL263 (3.63)	-
	-	-	-		-	ASN529 (3.86)	-
	-	-	-		-	TRP531 (3.75, 3.60, 3.64)	-
	-	-	-		-	-	ASP154 (3.95)

* Residues shows in red are catalytic residues and in green residues in the active site.[16–18] * residues were also found to interact with diminazene[16]

Based on the results obtained from molecular docking and comparing then to the experimental results, DockThor implicitly considering the protein flexibility was found as the best option.

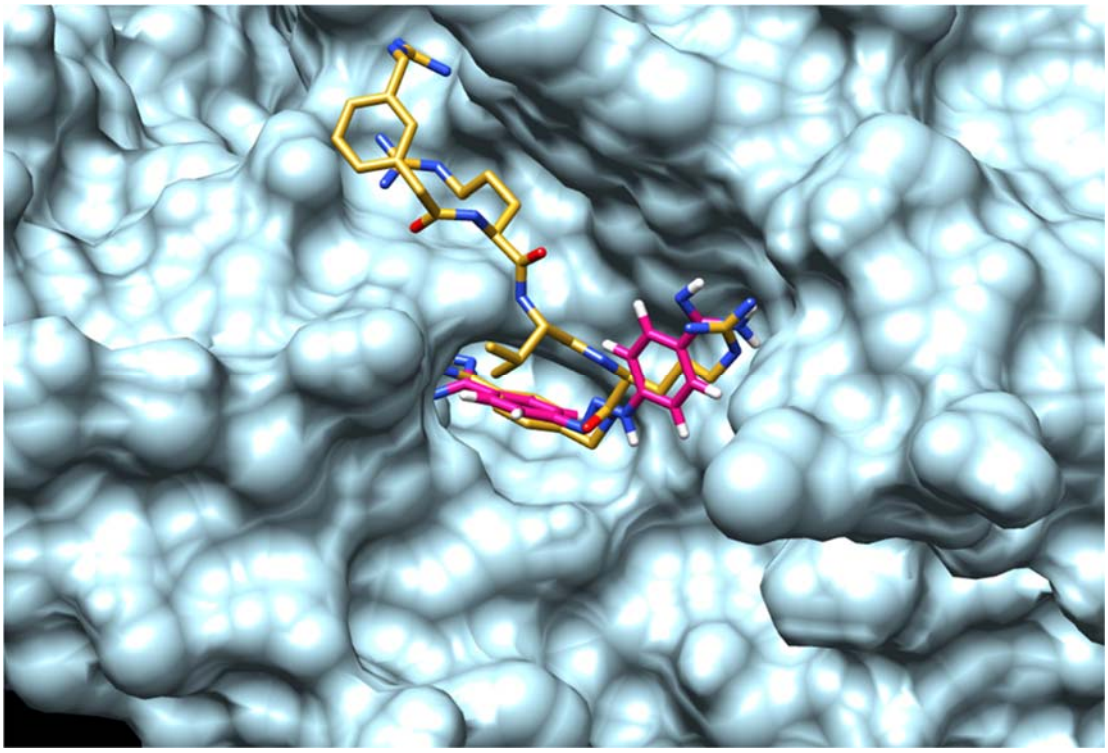

Figure S8-3. Binding mode of diminazene (pink) and the original ligand MI-52[19] (gold) in the furin (PDB code 5JXH) catalytic/binding site. Picture was made using UCSF Chimera 1.15.[9]

References

(1) Colovos, C., Yeates, T. O. (1993) Verification of Protein Structures: Patterns of Nonbonded Atomic Interactions. *Protein Sci. 2* (9), 1511–1519.

(2) Laskowski, R. A., MacArthur, M. W., Moss, D. S., Thornton, J. M. (1993) PROCHECK: A Program to Check the Stereochemical Quality of Protein Structures. *J. Appl. Crystallogr. 26* (2), 283–291.

(3) Guex, N., Peitsch, M. C. (1997) SWISS-MODEL and the Swiss-PdbViewer: An Environment for Comparative Protein Modeling. *Electrophoresis 18* (15), 2714–2723.

(4) Idris, M. O., Yekeen, A. A., Alakanse, O. S., Durojaye, O. A. (2020) Computer-Aided Screening for Potential TMPRSS2 Inhibitors: A Combination of Pharmacophore Modeling, Molecular Docking and Molecular Dynamics Simulation Approaches. *J. Biomol. Struct. Dyn. Jul* 16, 1–19.

(5) Zhu, H., Du, W., Song, M., Liu, Q., Herrmann, A., Huang, Q. (2021) Spontaneous Binding of Potential COVID-19 Drugs (Camostat and Nafamostat) to Human Serine Protease TMPRSS2. *Comput. Struct. Biotechnol. J. 19*, 467–476.

(6) Brooke, G. N., Prischi, F. (2020) Structural and Functional Modelling of SARS-CoV-2 Entry in Animal Models. *Sci. Rep. 10* (1), 15917.

(7) Chikhale, R. V., Gupta, V. K., Eldesoky, G. E., Wabaidur, S. M., Patil, S. A., Islam, M. A. (2020) Identification of Potential Anti-TMPRSS2 Natural Products through Homology Modelling, Virtual Screening and Molecular Dynamics Simulation Studies. *J. Biomol. Struct. Dyn. Aug* 3, 1–16.

(8) Choi, Y., Shin, B., Kang, K., Park, S., Beck, B. R. (2020) Target-Centered Drug Repurposing Predictions of Human Angiotensin-Converting Enzyme 2 (ACE2) and Transmembrane Protease Serine Subtype 2 (TMPRSS2) Interacting Approved Drugs for Coronavirus Disease 2019 (COVID-19) Treatment through a Drug-Target Interaction Deep Learning Model. *Viruses 12* (11), 1325.

(9) Pettersen, E. F., Goddard, T. D., Huang, C. C., Couch, G. S., Greenblatt, D. M., Meng, E. C., Ferrin, T. E. (2004) UCSF Chimera - A Visualization System for Exploratory Research and Analysis. *J. Comput. Chem. 25* (13), 1605–1612.

(10) Trott, O., Olson, A. J. (2009) AutoDock Vina: Improving the Speed and Accuracy of Docking with a New Scoring Function, Efficient Optimization, and Multithreading. *J. Comput. Chem. 31* (2), 455–461.

(11) Grosdidier, A., Zoete, V., Michielin, O. SwissDock, a Protein-Small Molecule Docking Web Service Based on EADock DSS. *Nucleic Acids Res.* **2011**, *39* (SUPPL. 2). https://doi.org/10.1093/nar/gkr366.

(12) Santos, K. B., Guedes, I. A., Karl, A. L. M., Dardenne, L. E. (2020) Highly Flexible Ligand Docking: Benchmarking of the DockThor Program on the LEADS-PEP Protein-Peptide Data Set. *J. Chem. Inf. Model. 60* (2), 667–683.

(13) Lohning, A. E., Levonis, S. M., Williams-Noonan, B., Schweiker, S. S. A Practical Guide to Molecular Docking and Homology Modelling for Medicinal Chemists. *Curr. Top. Med. Chem.* **2017**, *17* (18), 2023–2040.

(14) dos Santos, R. N., Ferreira, L. G., Andricopulo, A. D. Practices in Molecular Docking and Structure-Based Virtual Screening. In *Computational Drug Discovery and Design. Methods in Molecular Biology*, Gore M., Jagtap U., Eds., Humana Press Inc.: New York, 2018, Vol. 1762, pp 31–50.

(15) Ferreira, L. G., Dos Santos, R. N., Oliva, G., Andricopulo, A. D. (2015) Molecular Docking and Structure-Based Drug Design Strategies. *Molecules 20* (7), 13384–13421.

(16) Wu, C., Zheng, M., Yang, Y., Gu, X., Yang, K., Li, M., Liu, Y., Zhang, Q., Zhang, P., Wang, Y., Wang, Q., Xu, Y., Zhou, Y., Zhang, Y., Chen, L., Li, H. (2020) Furin: A Potential Therapeutic Target for COVID-19. *iScience 23* (10), 101642.

(17) Dahms, S. O., Hardes, K., Becker, G. L., Steinmetzer, T., Brandstetter, H., Than, M. E. (2014) X-Ray Structures of Human Furin in Complex with Competitive Inhibitors. *ACS Chem. Biol. 9* (5), 1113–1118.

(18) Dahms, S. O., Jiao, G. S., Than, M. E. (2017) Structural Studies Revealed Active Site Distortions of Human Furin by a Small Molecule Inhibitor. *ACS Chem. Biol. 12* (5), 1211–1216.

(19) Dahms, S. O., Arciniega, M., Steinmetzer, T., Huber, R., Than, M. E. (2016) Structure of the Unliganded Form of the Proprotein Convertase Furin Suggests Activation by a Substrate-Induced Mechanism. *Proc. Natl. Acad. Sci. U. S. A. 113* (40), 11196–11201.